Egypt. J. Chem. **Vol. 67**, No. 12 pp. 245 - 252 (2024)

Egyptian Journal of Chemistry

http://ejchem.journals.ekb.eg/

Isotherm Models for Metal Removal Using Modified Graphene

Soha W. Hgag[1], Shimaa M. Abdel Moniem[1], Mohammed Eid M. Ali[1] , Magdy K. Zahran[*2], Ahmed Barhoum[2], Hanan S. Ibrahim[1]

[1] *Water Pollution Research Department, Environmental and Climate Changes Institute, National Research Centre, El-Buhouth St., Dokki, Cairo, P.O. 12622, Egypt*

[2] *Chemistry Department, Faculty of Science, Helwan University, Ain-Helwan, Cairo, P.O. 11795, Egypt*

Abstract

In the present study, a holey graphene oxide (HGO) was synthesized by a fast-designed method via carbonization of apricot shell waste. Raman spectroscopic analysis confirmed the structure of HGO. A simple adsorption method was designed for the removal of La^{3+} and Ni^{2+} by the utilization of HGO. The adsorption rate of La^{3+} progressively reached its maximum after 5 min, while the maximum adsorption of Ni^{2+} ions was achieved after 90 min. The adsorption isotherm data exhibited the best fitting with Langmuir isotherm for the adsorption of La^{3+} and Ni^{2+} with a correlation coefficient (0.9985, 0.9986), and the adsorption is considered to be favourable with a separation factor $0 < R_L < 1$, which confirms that the adsorption process takes place on heterogeneous surface adsorbent, which is consistent with HGO nature. This model assumes that adsorption sites increase exponentially with adsorption, resulting in multilayer adsorption. This study suggested that the HGO has proved to be an efficient adsorbent for $Ni^{2+}$and La^{3+} ions removal from aqueous solutions.

Keywords: Holey graphene oxide , Adsorption, Wastewater, Metal ions, Adsorption isotherm

1. Introduction

With the development of the global economy and increasing water demand, the shortage of water resources is becoming more serious due to environmental pollution, and access to clean water without various organic and inorganic pollutants in aquatic ecosystems has become a worldwide issue (Liu et al., 2023). Recently, effective regenerable freshwater technologies have been the focus of numerous efforts (W. Li et al., 2020a; Qasim et al., 2019; Youssef et al., 2024).

The increasing digitalization and complexity of modern goods drive the growing demand for specialty metals, with the imbalance between projected supply and demand accentuated by geopolitical supply risks resulting in the identification of certain metals as ‘‘critical.” (European Commission, 2020). Multiple of these critical metals are found in battery technologies such as nickel metal hydride (NiMH) batteries, which contain an important concentration of lighter rare earth elements (REEs) (Zhang et al., 2018)

Lanthanum (La) is the most widely used REE in the manufacture of NiMH batteries due to its high hydrogen storage capacity, with concentrations ranging between 18 and 28 wt.% depending on the anode chemistry, namely AB5 type (A : REEs (La); B :z Al, Co, Ni, and Mn). These end-of-life batteries will require adequate treatment once disposed of to both recover their inherent metallic value and minimize their potential environmental impact (Fila et al., 2019).

*Corresponding author e-mail: zahranmk@science.helwan.edu.eg.;(Magdy K. Zahran).
Received date 15 January 2024 ; Revised date 18 February 2024 ; Accepted date 01 March 2024
DOI10.21608/ejchem.2024.263118.9195

Adsorption has been widely applied for the separation and treatment of heavy metals from their waste and/or wastewater due to its low cost, superficial handling of materials, ability for energy recovery, and eco-friendliness, i.e., green algae, waste factories tea, and seaweeds (Elmoubarki et al., 2015), loofa sponge-immobilized biomass of chlorella sorokinian, aerobic activated sludge, spent animal bones (Burakov et al., 2018), fly ash (Hussain, 2018), activated carbon (Iwahori et al., 2014), crab shell (Botelho Junior et al., 2019), and sugar industry waste (Tohamy et al., 2020; Ali, et al., 2022).

However, adsorbent materials' low adsorption efficiency in the removal of heavy metal ions limited their applications. Thus, exploring novel adsorbents with higher adsorption capacity has been a significant demand. In addition, the use of sustainable composites has introduced numerous advantages in terms of low cost, low density, and low energy consumption compared to synthetic materials (Kamel et al., 2020; Kazemnejadi et al., 2019).

The core objective of the current work is to delve into the preparation of holy graphene oxide (HGO) and explore its efficacy for remediation of precious metal contaminant from aqueous solution. The structural features of HGO were examined. The adsorption behavior of lanthanum (La^{3+}) and nickel (Ni^{2+}) onto HGO was optimized comprehensively under various experimental conditions (e.g. HGO dosage, adsorbent concentration, and contact time). Comprehending of adsorption mechanism of lanthanum and nickel onto HGO was facilitated through modelling of different isotherms assumptions. Moreover, the feasibility for HGO to be functioned as a highly effective adsorbent material is targeted. The work aims to apply as-prepared HGO for metal removal from aqueous solution.

2. Experimental

2.1. Materials and Methods

All metal salts used throughout the work were of analytical reagent grade and were used without further purification. Stock solutions of Ni^{2+} and La^{3+} ions were prepared in deionized water from nickel chloride hexahydrate ($NiCl_2.6H_2O$) and lanthanum carbonate decahydrate [$(La_2(CO_3)_3.\ 10\ H_2O$], all of them Fisher chemicals. Nitric acid (65% HNO_3; Merck) was used for heavy metal digestion.

2.2. Preparation of apricot shell holy graphene oxide (HGO)

Apricot shell was used as a simple and cost-effective method for the preparation of holey graphene nanosheets. For HGO synthesis, apricot shell was first dried for 2 h at 105°C. After that, the shells were grounded to obtain powder. Then, the powder waste material is carbonized in a muffle furnace under N_2 gas flow for 1 h at 900°C, and a gradual decrease in temperature during cooling is left for 3 h under N_2 gas flow. The carbonization is conducted in the fume hood, which is equipped with an integrated filter through charcoal for the adsorption of hazardous emissions (Lokhande et al., 2020).

2.3. Metal adsorption studies

Batch metal adsorption studies were conducted in Erlenmeyer conical flask using different doses of Apricot shells Holy graphene oxide (HGO) (0.6 - 2g) in 1L of different concentration ranged from 2 to 80 mg/L of Nickel, and lanthanum solution separately. The experiments were carried out at the actual pH of the solution.

The solutions were subjected to filtration via a 0.45 µm syringe membrane. The concentrations of metal ions were analysed using inductively coupled plasma optical emission spectrometry (Agilent ICP-OES 5100, Australia Synchronous Vertical Dual View (SVDV), after calibration with a series of nickel and lanthanum solutions.

Nickel and lanthanum concentrations in the samples were measured using triplicate analysis. Each set of measurements was fitted using a five-point calibration curve. The accuracy of Ni^{+2} and La^{+3} readings was measurements by using the quality control standards.

The removal percentage of La^{+3} and Ni^{+2} ions (R%) was calculated using Eq. (1) as follows:

$$\mathbf{R} = \frac{C_o - C_e}{C_o} \times \mathbf{100\ \%} \quad \text{..... (1)}$$

Where,
C_o: initial metal concentration (mg/L),
C_e: equilibrium or final metal concentration in the solution.

The equilibrium adsorption capacity q_e (mg/g), i.e., quantity of metals adsorbed by unit mass of HGO, was determined according to the following equation:

$$q_e = (C_o - C_e) \times \frac{V}{m} \quad \text{..... (2)}$$

Where,
q_e: metal adsorbed at equilibrium (mg/g),

m: adsorbent mass (g),
V: solution volume in (L).

3. Results and Discussion

3.1. Characterization of the prepared HGO using Raman analysis

The Raman spectrum of the HGO product was displayed in **Fig. 1**. As shown, three main peaks are presented, i.e., the D-band (1355 cm^{-1}), the G-band (1596 cm^{-1}), and the 2D-band (2910 cm^{-1}). Indeed, these values are too close to those recorded for graphene, which indicates that the obtained carbon is graphene-like. The pronounced G-band confirmed the sp^2-hybridized carbon atoms. (Yeleuov et al., 2021). Meanwhile, the D-band and the 2D-band indicate the structure defects present in graphene and the number of graphene layers obtained. In depth, the ratio of D and G band intensities (I_D/I_G) reflects the disorder of the produced graphene, i.e, the lower the D-band intensity, the higher the ordered structure. As stated, graphite has the weakest structure disorder among carbonaceous materials (Ghanem & Rehim, 2018) $I_D/I_G \sim 0.2$. The obtained graphene-like showed ~ 0.8 of the D:G intensities ratio. This means that the obtained graphene is characterized by high structural defects and disorder, which might be favorable for some applications, e.g., water treatment. Moreover, an increase in the G-band intensity compared with that of the 2D-band confirmed the presence of graphene multilayers. Accordingly, it can be claimed with confidence that the method used in this study paves the way to obtaining graphene-like structures (Ghanem et al., 2020).

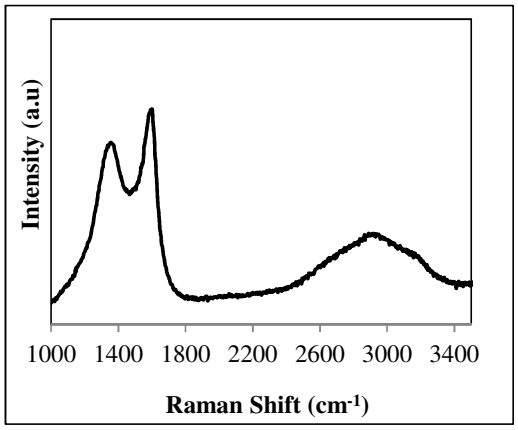

Figure 1: Raman spectrum spectra of apricot shell and HGO after carbonization at 900°C under nitrogen

3.2. Adsorption process for metals

3.2.1. Effect of contact time on La^{3+} and Ni^{2+} adsorption on apricot driven HGO

Fig. 2 represents the change in removal efficiency of La^{3+} and Ni^{2+} with time, where the equilibrium time reached for the removal of La^{3+} and Ni^{2+} by HGO composite powder was rapid. The adsorption rate of La^{3+} progressively reached its maximum after 5 min with a noticeable that the removal efficiency reached the maximum of 99 %, and then the percentage of the removal slightly decreased after 10 min. Meanwhile, the percentage of the removal for Ni^{2+} was progressively increased with time, and equilibrium was achieved after 90 min.

Fig. 2 also illustrates that the removal efficiency percentage for Ni rose from 18% after 5 minutes of contact time to 80% after 90 minutes of contact time. The removal of La^{3+} ions occur clearly in a short period.

3.2.2. Effect of HGO dosage on the removal of La^{3+} and Ni^{2+}.

The impact of HGO dosages ranging from 0.6 to 2 g/L was investigated for La^{3+} and Ni^{2+} removal at the optimal period (5, 30 min), respectively. The pH was set at 3.5 and 6.70, with starting concentrations of La^{3+} and Ni^{2+} ions of 2 and 10 mg/L, respectively. The results in **Fig. 2** show that increasing the adsorbent dosage from 0.6 to 2 g/L improved the proportion of La^{3+} removed, reaching 90%.

These findings are explained by the fact that increasing the adsorbent dose gradually increases the adsorption sites available for La^{3+} and Ni^{2+} removal (Gao et al., 2021; Gupta, S., & Kumar, 2019). Increasing the adsorbent dose to 2 g/L causes inconsistent adsorption and decreases to~60%. This might be attributable to oversaturation of the adsorbent's attachment sites, which is caused by La^{3+} and Ni^{2+} ions overcrowding on the sites (Menazea et al., 2020; Rezania et al., 2022). As a result, throughout the rest of the batch studies, 1g/L of the adsorbent dose was employed as the operational dosage.

The HGO adsorption capacity equilibrium (q_e) for La^{3+} diminished from 2.4 to 0.7, and for Ni^{2+} from 9.7 to 2.5 mg/g, as the dose of HGO composite powder increased from 0.6 to 2 g/L. The rise in HGO dosage, while maintaining constant concentrations of La^{3+} and Ni^{2+} ions, may explain the reduction in the amount of La^{3+} and Ni^{2+} ions adsorbed per unit mass, attributed to the decreased availability of these ions per unit mass of the adsorbent (Li et al., 2020b; Sayed et al., 2019).

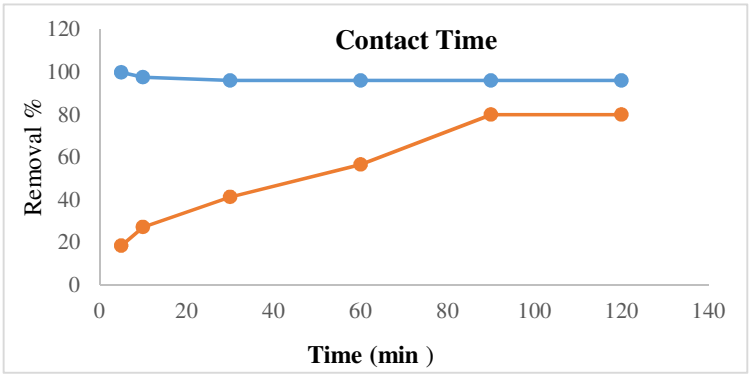

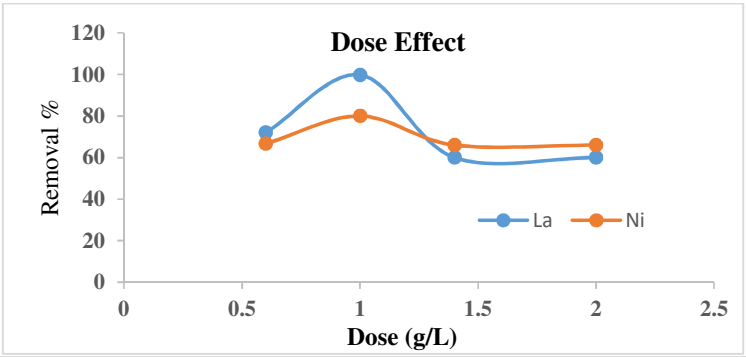

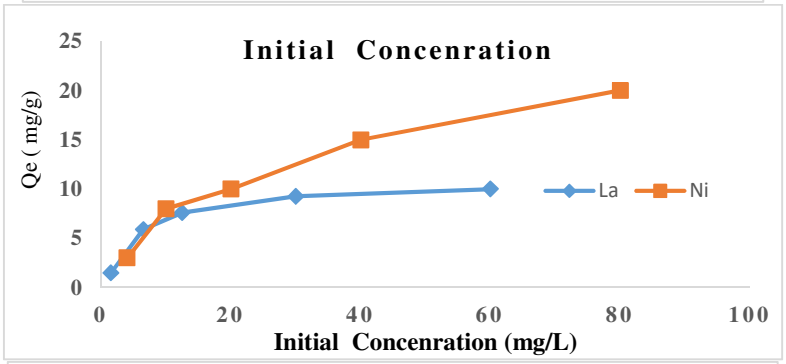

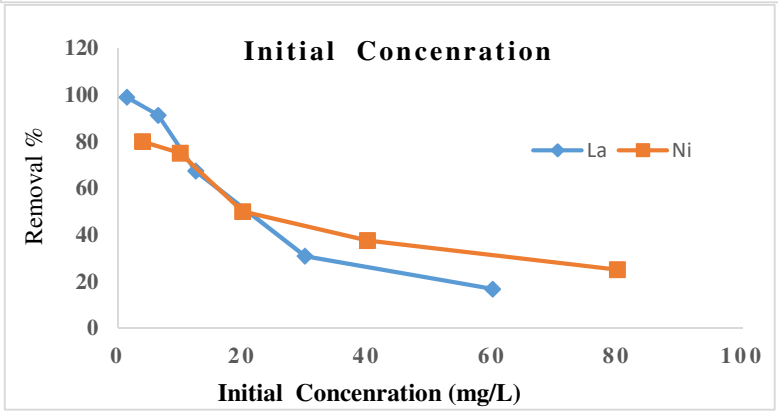

Figure 2: Different factors effect on adsorption of La^{3+} and Ni^{2+} over HGO

3.2.3. Effect of initial metal concentrations on adsorption of apricot HGO

The effect of initial La^{3+} and Ni^{2+} ion concentrations on its adsorption was investigated by mixing 1 g of HGO composite powder with 1L of lanthanum and nickel solutions ranging from 2 to 80 mg/L at the optimum time operating conditions for each metal ion. With different initial concentrations of La^{3+} and Ni^{2+} in the solution, the adsorption capacity and removal efficiency of the HGO composite powder are displayed in **Fig. 2**. The adsorption capacity of HGO composite powder increased linearly with increasing initial La^{3+} and Ni^{2+} ion concentrations until reaching a saturation value of 60, 80 mg/L (qe is 10.08, 20 mg/g), respectively. This might be because the available adsorption surface and active sites are fully utilized (Aldalbahi et al., 2020; Meng et al., 2022). While the metal ion concentration increased from 2 to 80 mg/L, the removal percentage of La^{3+} and Ni^{2+} ions declined from 99 to 20%, and 80 to 25%, respectively. Wherever the ion concentration of La^{3+} and Ni^{2+} increased, the available adsorption sites of the adsorbent material get saturated and become fewer consequently, the percentage of La^{3+} and Ni^{2+} ions removed decreased as the initial metal ion concentration increased (Cherono et al., 2021; Nodeh et al., 2020).

3.2.4. Isotherms model for the adsorption process

The equilibrium adsorption data may enhance comprehension of the interaction between adsorbate and adsorbent, as well as facilitate the design and execution of the adsorption process. Therefore, isothermal models were applied for the data analysis. In this work, two models are used to explore the single-solute adsorption process: Freundlich and Langmuir isotherms.

3.2.4.1. Langmuir isotherm for the adsorption of La^{3+} and Ni^{2+} by HGO

The Langmuir model assumes that the adsorbent has a homogenous surface and that all adsorbent sites have equal affinity to the adsorbate(Mohammed et al., 2014), as well as that there is no interaction between adsorbate molecules. The equation is as follows (Maamoun et al., 2021) :

$$C_e/q_e = 1/(b.q_{max}) + C_e/q_{max} \quad \text{..... (3)}$$

Where C_e (mg/L) represents the equilibrium concentration of the solute, q_e (mg/g) is the amount of La^{3+} and Ni^{2+} adsorbed per unit mass of the HGO adsorbent, q_{max} (mg/g) represents the maximum adsorption capacity, and b (L/mg) is the Langmuir constant. q_{max} and b is calculated by the linear plots of Ce/q_e against Ce.

Fig. 3 illustrates the Langmuir isotherm for the adsorption of La^{3+} and Ni^{2+} by HGO, whereas **Table 1** enumerates the computed parameters. The elevated correlation value (R^2 = 0.9985, 0.9986) and the Langmuir maximum adsorption capacities of q_{max} 10.08 and 25.19 mg/g, respectively, substantiate the heterogenous coverage with chemisorption of La^{3+} and Ni^{2+} onto the adsorbent surface (Aldalbahi et al., 2020; Gupta & Kumar, 2019; Marwani et al., 2017). The R_L is a dimensionless constant separation factor that defines the key attributes of the Langmuir adsorption isotherm model. R_L is articulated in the subsequent equation:

$$R_L = \frac{1}{1+K_L C_0} \quad \text{..... (4)}$$

where K_L is the Langmuir constant (mg/g), and C_0 is the adsorbate initial concentration.

The result shows that R_L for La = 0.07842 and R_L for Ni = 0.3428, which means that the adsorption is considered favourable

($0< R_L<1$) (Ayawei et al., 2017).

3.2.4.2. Freundlich isotherm model for the adsorption of La^{3+} and Ni^{2+} by HGO

The Freundlich isotherm model posits that when adsorption sites become completely occupied, the adsorption energy declines exponentially. The Freundlich isotherm represents adsorption on a heterogeneous surface as well as interactions between adsorbed molecules (multilayer adsorption). Freundlich equation can be expressed in linear form as follows (Sabri et al., 2015):

$$\log q_e = \log K_f + 1/n \log C_e \quad \text{..... (5)}$$

In this context, *qe* denotes the equilibrium adsorption capacity (mg/g), *Ce* signifies the equilibrium concentration of La^{3+} and Ni^{2+} in solution (mg/L), *kf* indicates a Freundlich constant associated with adsorption capacity, and n represents the adsorption intensity, which is another Freundlich constant related to adsorption intensity. *Kf* and n may be ascertained from the intercept and slope of the linear graph of ln *qe* vs log *Ce*.

The results shown in Fig. 3 and Table 1 indicate that the experimental data closely align with the Freundlich model, exhibiting R^2 values of 0.99 and 0.989. A value of n above one signifies a strong affinity between HGO and La^{3+} and Ni^{2+} ions, indicating chemical adsorption. The *kf* values were 6.32 and 4.17, indicating the adsorption capacity of the adsorbent; a larger value signifies superior ability to adsorb La^{3+} and Ni^{2+} ions in the solution, respectively (Aldalbahi et al., 2020b; Gupta,S., & Kumar, 2019; Marwani et al., 2017b).

The current findings reveal that the values of n for La^{3+} is 8.3 and for Ni^{2+} is 2.5, both of which are within the range of 2 to 10, signifying a strong adsorption capacity (Yao et al., 2011). The elevated R value for Langmuir and Freundlich isotherms over 0.98 signifies that the adsorption sites are heterogeneous.

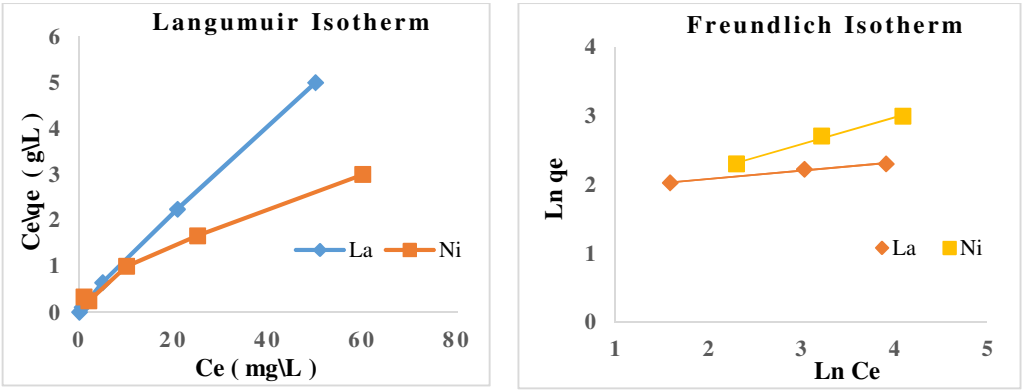

Figure 3: Different isotherm models for the adsorption of Ni^{2+} and La^{3+} ions onto HGO

Table 1: Different isotherm model equations, parameters, and its values for the adsorption of Ni^{2+} and La^{3+} ions onto HGO

Isotherm models	Equation	Parameters	Value	
			La^{3+}	Ni^{2+}
Langmuir	$\frac{c_e}{q_e} = \frac{1}{k_L q_{max}} + \frac{c_e}{q_{max}}$	K_L *L/mg*	1.1657	0.0627
		q_{max}	10.08	25.19
		R^2	0.9985	0.9986
		R_L	0.07842	0.3428
Freundlich	$ln\, q_e = ln\, k_F + \frac{1}{n} ln\, c_e$	K_f *mg/g*	6.32	4.17
		n	8.340	2.582
		R^2	0.9981	0.989

Conclusion

Green Holey graphene oxide (HGO) leads to a promising structure for the removal of $La^{3+}$and Ni^{2+} within a noticeably brief time. The HGO may achieve an efficiency of up to 80 % for the removal of La^{3+} and Ni^{2+} when they are present individually in solution. The maximum removal of La^{3+} and Ni^{2+} among the examined agricultural wastes was seen for HGO derived from apricot shell. The removal efficiency peaked at 99% after 5 minutes and attained 80 % after 90 minutes of contact time, with nickel ions adsorption aligning well with the Langmuir isotherm model. Lanthanum adsorption demonstrated strong concordance

with both isotherm models, as evidenced by the elevated R^2 values for the Langmuir and Freundlich isotherms, above 0.98, which suggests that the adsorption sites are heterogeneous the Langmuir maximum adsorption capacity for the adsorption of La^{3+} and Ni^{2+} by HGO, were q_{max} 10.08 and 25.19 mg/g, respectively.

References

Aldalbahi, A., El-naggar, M., Khattab, T., Abdelrahman, M., Rahaman, M., Alrehaili, A., & El-newehy, M. (2020). Development of green and sustainable cellulose acetate/graphene oxide nanocomposite films as efficient adsorbents for wastewater treatment. *Polymers*,*12*(11),1–16. https://doi.org/10.3390/polym12112501

Ayawei, N., Ebelegi, A. N., & Wankasi, D. (2017). Modelling and Interpretation of Adsorption Isotherms. In *Journal of Chemistry* (Vol. 2017).Hindawi.Limited. https://doi.org/10.1155/2017/3039817

Cherono, F., Mburu, N., & Kakoi, B. (2021). Adsorption of lead, copper and zinc in a multi-metal aqueous solution by waste rubber tires for the design of single batch adsorber. *Heliyon*,*7*(11). https://doi.org/10.1016/j.heliyon.2021.e08254

European commission. (2020). *European Commission,2020.* https://ec.europa.eu/eu2020/pdf/COMPLET%20EN%20BARROSO%20%20%20007%20-%20Europe%202020%20%20EN%20version.pdf

Fila, D., Hubicki, Z., & Kołodyńska, D. (2019). Recovery of metals from waste nickel-metal hydride batteries using multifunctional Diphonix resin. *Adsorption*, *25*(3), 367–382. https://doi.org/10.1007/s10450-019-00013-9

Gao, C., Wang, X. L., An, Q. Da, Xiao, Z. Y., & Zhai, S. R. (2021). Synergistic preparation of modified alginate aerogel with melamine/chitosan for efficiently selective adsorption of lead ions. *Carbohydrate Polymers*, *256*. https://doi.org/10.1016/j.carbpol.2020.117564

Ghanem, A. F., Badawy, A. A., Mohram, M. E., & Abdel Rehim, M. H. (2020). Synergistic effect of zinc oxide nanorods on the photocatalytic performance and the biological activity of graphene nano sheets. *Heliyon*, *6*(2). https://doi.org/10.1016/j.heliyon.2020.e03283

Gupta, S., & Kumar, A. (2019). Removal of nickel (II) from aqueous solution by biosorption on A. barbadensis Miller waste leaves powder. *Applied.Water.Science*,*9*(4). https://doi.org/10.1007/s13201-019-0973-1

Li, S. S., Song, Y. L., Yang, H. R., An, Q. Da, Xiao, Z. Y., & Zhai, S. R. (2020). Modifying alginate beads using polycarboxyl component for enhanced metal ions removal. *International Journal of Biological Macromolecules*, *158*, 493–501. https://doi.org/10.1016/j.ijbiomac.2020.05.038

Lokhande, A. C., Qattan, I. A., Lokhande, C. D., & Patole, S. P. (2020). Holey graphene: An emerging versatile material. In *Journal of Materials Chemistry A* (Vol. 8, Issue 3, pp. 918–977). Royal Society of Chemistry. https://doi.org/10.1039/c9ta10667g

Maamoun, I., Eljamal, R., Falyouna, O., Bensaida, K., Sugihara, Y., & Eljamal, O. (2021). Insights into kinetics, isotherms and thermodynamics of phosphorus sorption onto nanoscale zero-valent iron. *Journal of Molecular.Liquids*,*328*. https://doi.org/10.1016/j.molliq.2021.115402

Marwani, H. M., Albishri, H. M., Jalal, T. A., & Soliman, E. M. (2017a). Study of isotherm and kinetic models of lanthanum adsorption on activated carbon loaded with recently synthesized Schiff's base. *Arabian Journal of Chemistry*,*10*,S1032–S1040. https://doi.org/10.1016/j.arabjc.2013.01.008

Marwani, H. M., Albishri, H. M., Jalal, T. A., & Soliman, E. M. (2017b). Study of isotherm and kinetic models of lanthanum adsorption on activated carbon loaded with recently synthesized Schiff's base. *Arabian Journal of Chemistry*,*10*,S1032–S1040. https://doi.org/10.1016/j.arabjc.2013.01.008

Menazea, A. A., Ezzat, H. A., Omara, W., Basyouni, O. H., Ibrahim, S. A., Mohamed, A. A., Tawfik, W., & Ibrahim, M. A. (2020). Chitosan/graphene oxide composite as an effective removal of Ni, Cu, As, Cd and Pb from wastewater. *Computational and Theoretical.Chemistry*,*1189*. https://doi.org/10.1016/j.comptc.2020.112980

Mohammed, M. I., Abdul Razak, A. A., & Hussein Al-Timimi, D. A. (2014). Modified multiwalled carbon nanotubes for treatment of some organic dyes in wastewater. *Advances in Materials Science and Engineering*, *2014*. https://doi.org/10.1155/2014/201052

Nodeh, M. K. M., Bidhendi, G. N., Gabris, M. A., Akbari-Adergani, B., Nodeh, H. R., Masoudi, A., & Shahabuddin, S. (2020). Strontium oxide decorated iron oxide

activated carbon nanocomposite: A new adsorbent for removal of nitrate from well water. *Journal of the Brazilian Chemical Society*, *31*(1), 116–125. https://doi.org/10.21577/0103-5053.20190138

Rezania, S., Mojiri, A., Park, J., Nawrot, N., Wojciechowska, E., Marraiki, N., & Zaghloul, N. S. S. (2022). Removal of lead ions from wastewater using lanthanum sulfide nanoparticle decorated over magnetic graphene oxide. *Environmental Research*, *204*. https://doi.org/10.1016/j.envres.2021.111959

Sabri, A. A., Albayati, T. M., & Alazawi, R. A. (2015). Synthesis of ordered mesoporous SBA-15 and its adsorption of methylene blue. *Korean Journal of Chemical Engineering*, *32*(9), 1835–1841. https://doi.org/10.1007/s11814-014-0390-y

Sayed, M., Abbas, M., Abdel Moniem, S. M., Ali, M. E. M., & Naga, S. M. (2019). Facile and Room Temperature Synthesis of Superparamagnetic Fe 3 O 4 /C Core/Shell Nanoparticles for Efficient Removal of Pb(II) From Aqueous Solution. *ChemistrySelect*, *4*(6), 1857–1865. https://doi.org/10.1002/slct.201803939

Yeleuov, M., Daulbayev, C., Taurbekov, A., Abdisattar, A., Ebrahim, R., Kumekov, S., Prikhodko, N., Lesbayev, B., & Batyrzhan, K. (2021). Synthesis of graphene-like porous carbon from biomass for electrochemical energy storage applications. *Diamond and Related.Materials*,*119*. https://doi.org/10.1016/j.diamond.2021.108560

Zhang, X., Li, L., Fan, E., Xue, Q., Bian, Y., Wu, F., & Chen, R. (2018). Toward sustainable and systematic recycling of spent rechargeable batteries. In *Chemical Society Reviews* (Vol. 47, Issue 19, pp. 7239–7302). Royal Society of Chemistry. https://doi.org/10.1039/c8cs00297e